AMERICAN SOCIETY FOR MICROBIOLOGY | Antimicrobial Agents and Chemotherapy®

Active-Site Protonation States in an Acyl-Enzyme Intermediate of a Class A β-Lactamase with a Monobactam Substrate

Venu Gopal Vandavasi,[a] Patricia S. Langan,[a] Kevin L. Weiss,[a] Jerry M. Parks,[b] Jonathan B. Cooper,[c] Stephan L. Ginell,[d] Leighton Coates[a]

Biology and Soft Matter Division, Oak Ridge National Laboratory, Oak Ridge, Tennessee, USA[a]; Biosciences Division, Oak Ridge National Laboratory, Oak Ridge, Tennessee, USA[b]; Birkbeck University of London, London, United Kingdom[c]; Structural Biology Center, Argonne National Laboratory, Argonne, Illinois, USA[d]

ABSTRACT The monobactam antibiotic aztreonam is used to treat cystic fibrosis patients with chronic pulmonary infections colonized by *Pseudomonas aeruginosa* strains expressing CTX-M extended-spectrum β-lactamases. The protonation states of active-site residues that are responsible for hydrolysis have been determined previously for the apo form of a CTX-M β-lactamase but not for a monobactam acyl-enzyme intermediate. Here we used neutron and high-resolution X-ray crystallography to probe the mechanism by which CTX-M extended-spectrum β-lactamases hydrolyze monobactam antibiotics. In these first reported structures of a class A β-lactamase in an acyl-enzyme complex with aztreonam, we directly observed most of the hydrogen atoms (as deuterium) within the active site. Although Lys 234 is fully protonated in the acyl intermediate, we found that Lys 73 is neutral. These findings are consistent with Lys 73 being able to serve as a general base during the acylation part of the catalytic mechanism, as previously proposed.

KEYWORDS β-lactamase, aztreonam, acyl-enzyme complex, neutron structure, X-ray structure

Received 29 July 2016 **Returned for modification** 30 August 2016 **Accepted** 29 September 2016

Accepted manuscript posted online 24 October 2016

Citation Vandavasi VG, Langan PS, Weiss KL, Parks JM, Cooper JB, Ginell SL, Coates L. 2017. Active-site protonation states in an acyl-enzyme intermediate of a class A β-lactamase with a monobactam substrate. Antimicrob Agents Chemother 61:e01636-16. https://doi.org/10.1128/AAC.01636-16.

Address correspondence to Leighton Coates, coatesl@ornl.gov.

β-lactam antibiotics inhibit bacterial cell wall biosynthesis by targeting penicillin-binding proteins (PBPs). The binding of β-lactam antibiotics to PBPs renders them chemically inert, causing bacterial cell death. To counter such powerful antimicrobials, bacteria have evolved to produce β-lactamase enzymes, which cleave the amide bond within the β-lactam ring via a general base hydrolysis mechanism (1–3). According to the Ambler classification (4), β-lactamases can be divided into four distinct groups (classes A to D). Classes A, C, and D consist of all serine-reactive hydrolases, whereas the class B enzymes are metalloenzymes that use a Zn^{2+}-bound water molecule to hydrolyze the amide bond of the β-lactam ring. Extended-spectrum β-lactamases (ESBLs) arose in the 1980s and exhibit increased hydrolytic activity against the first-, second-, and third-generation extended-spectrum cephalosporins and monobactams (3–6). Toho-1 β-lactamase, also classified as CTX-M-44, is a class A ESBL. Like most other class A β-lactamases, it comprises two highly conserved domains (α/β and α), with the active site located at the interface of these two domains (7, 8).

In contrast to most other β-lactams, which have at least two rings, in monobactams the β-lactam ring is not fused to another ring. Aztreonam has a large R group attached to the β-lactam ring that inhibits its hydrolysis by Toho-1 β-lactamase (9). The proposed catalytic mechanism of monobactam breakdown by a class A β-lactamase is shown in Fig. 1. After substrate binding, Ser 70 attacks the carbonyl carbon of the β-lactam ring to form an acyl-enzyme intermediate, which is then deacylated to liberate the inacti-

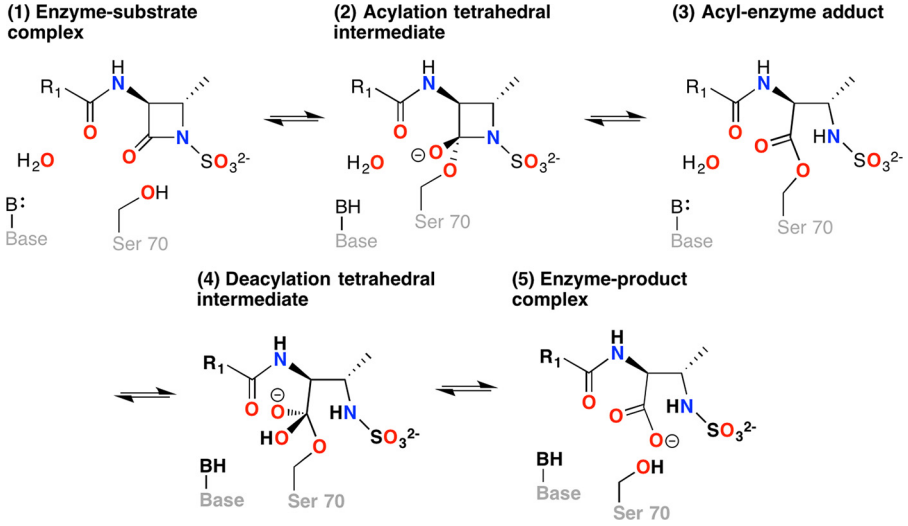

FIG 1 Catalytic cycle of a class A β-lactamase illustrated for a monobactam substrate. All class A β-lactamases employ an active site serine nucleophile to cleave the β-lactam bond of the substrate in a two-step acylation-deacylation reaction cycle that leads to overall hydrolysis. The acylation reaction initiates with the formation of a precovalent substrate complex (stage 1). A general base-catalyzed nucleophilic attack on the β-lactam carbonyl by the serine hydroxyl proceeds through a tetrahedral intermediate (stage 2) to form a transient acyl-enzyme adduct (stage 3). In the deacylation step, the acyl-enzyme adduct (stage 3) undergoes a general base-catalyzed attack by a hydrolytic water molecule to form a second tetrahedral intermediate (stage 4), which then collapses to form a postcovalent product complex (stage 5), from which the hydrolyzed product is released.

vated antibiotic (1, 2). Glu 166 plays a vital role in the deacylation step (Fig. 1, stages 3 to 5), where it acts as the activating base of a hydrolytic water molecule (10, 11). Mutating Glu 166 halts the reaction at the acyl intermediate (stage 3), allowing this state to be characterized structurally. Glu 166 has also been proposed to act as the catalytic base in the acylation step of the reaction (Fig. 1, stages 1 to 3) in which this residue deprotonates the hydroxyl of Ser 70 via a water molecule before Ser 70 attacks the carbonyl carbon of the β-lactam ring (8, 12, 13). Wild-type β-lactamases rapidly hydrolyze β-lactam antibiotics, making it virtually impossible to trap the acyl-enzyme intermediate.

It has been observed that Glu 166 mutants are still able to form acyl-enzyme intermediates, albeit with rate decreases of between 100-fold and 1,000-fold (11, 14, 15). This observation strongly suggests that Lys 73 can act as general base during the acylation step, as proposed in a number of studies (10, 11, 16, 17). Lys 73 is highly conserved throughout the serine-reactive β-lactamase families as well as the penicillin-binding proteins (18). This active-site residue is in close proximity to other catalytic residues, including Ser 70, Ser 130, and Glu 166. Mutation of Lys 73 to Arg results in a 100-fold decrease in acylation activity (19), indicating that Lys 73 participates in catalysis, although its role is still unclear. However, when both Lys 73 and Glu 166 are mutated, the rate constants for the acylation reaction decrease by 10,000-fold (19).

High-resolution X-ray structures have been determined previously for an Arg 274 Asn/Arg 276 Asn double mutant and a Glu 166 Ala/Arg 274 Asn/Arg 276 Asn triple mutant of Toho-1 β-lactamase in its apo form (20). The mutations Arg 274 Asn and Arg 276 Asn prevent crystal twinning and increase diffraction resolution (20) without dramatically affecting the kinetics of the enzyme (9). Neutron crystal structures have also been determined for both of these variants, clearly revealing that Lys 73 and Lys 234 are fully protonated and Glu 166 is anionic in the apoenzyme (21, 22). However, the protonation states of active-site residues in a monobactam acyl-enzyme intermediate have not yet been determined.

To characterize β-lactam hydrolysis in a class A β-lactamase, we determined both neutron and high-resolution 15 K X-ray acyl-intermediate structures of the Toho-1 Glu

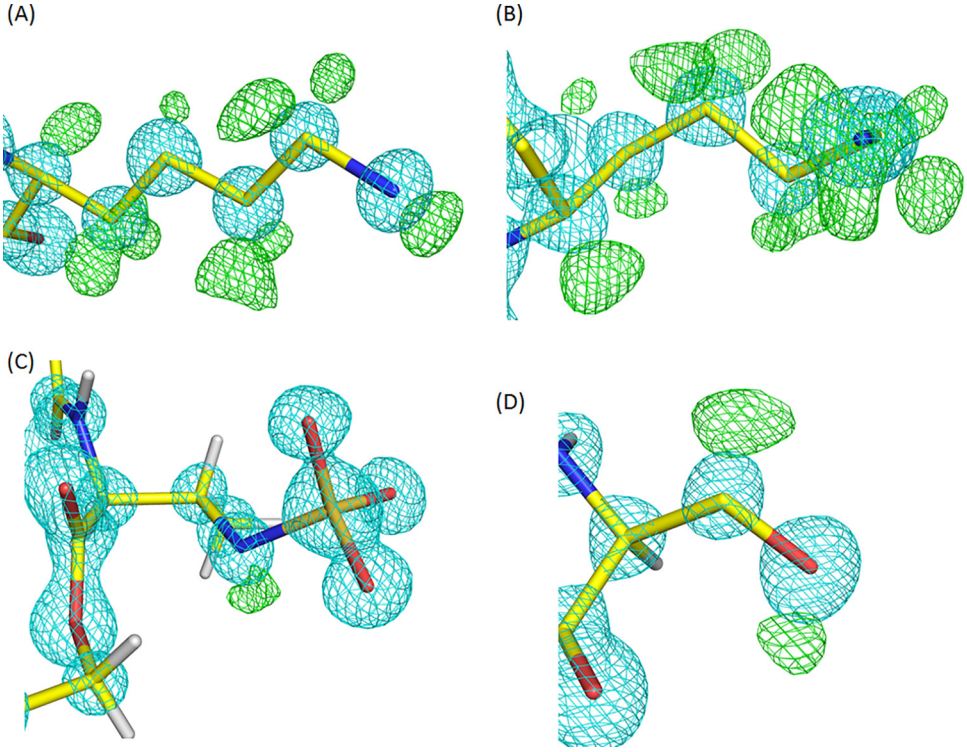

FIG 2 15 K X-ray electron density for key residues in the active site. The $2F_o$-F_c density at 3.7 σ is shown in cyan, and the F_o-F_c density at +2.5 σ is shown in green. Side-chain deuterium atoms have been omitted from (A) Lys 73, (B) Lys 234, (C) aztreonam, and (D) Ser 130 to elucidate their actual positions.

166 Ala/Arg 274 Asn/Arg 276 Asn mutant in complex with the monobactam antibiotic aztreonam, which is often used to treat bacterial lung infections in patients with cystic fibrosis (23). The aztreonam acyl intermediate was trapped for combined neutron and X-ray structure determination by mutating Glu 166 to Ala.

RESULTS AND DISCUSSION

The combination of neutron diffraction and 15 K X-ray diffraction enabled us to visualize most of the deuterium atoms within the active site of the monobactam antibiotic binding site. As a result, we probed the protonation states and hydrogen-bonding pattern therein, which allowed us to infer key aspects of the hydrolysis mechanism. In the 15 K X-ray structure, the average atomic displacement parameter (ADP) or B factor for protein main chain atoms is 7.68 Å^2, with an average of 12.92 Å^2 for protein side chain atoms. However, at around 5 Å^2, the values for the main-chain and side-chain ADPs of atoms in the three active site key residues, Lys 73, Ser 130, and Lys 234, are considerably lower than the average. Thus, we observed clear omit electron density for almost all of the deuterium atoms within the active site. The side chain of Lys 73 shows omit electron density for most of the deuterium atoms on the side chain (Fig. 2A). Omit electron density is present for both of the deuterium atoms on the C_β, C_δ, and C_ε atoms, but only a single deuterium is visible on C_γ. The omit electron density around N_ζ of Lys 73 is not as clear as on the rest of the side chain but seems to indicate that a hydrogen bond is formed with O_δ of Asn 132 (2.90 Å). It also suggests the presence of a hydrogen bond (2.90 Å) with the main-chain carbonyl oxygen of Ser 130. The omit electron density for the side chain of Lys 234 confirms that it is in the ND3+ cationic form and reveals the positions of all three deuterium atoms (Fig. 2B). It forms hydrogen bonds with O_γ of Ser 130 (2.84 Å), the main-chain carbonyl oxygen of Thr 235 (2.83 Å), and a nearby water molecule (2.73 Å). The omit electron density around the β-lactam ring nitrogen of aztreonam clearly indicates that it is protonated, with the deuterium orientated toward O_γ of Ser 130, with which it forms a hydrogen bond (2.84

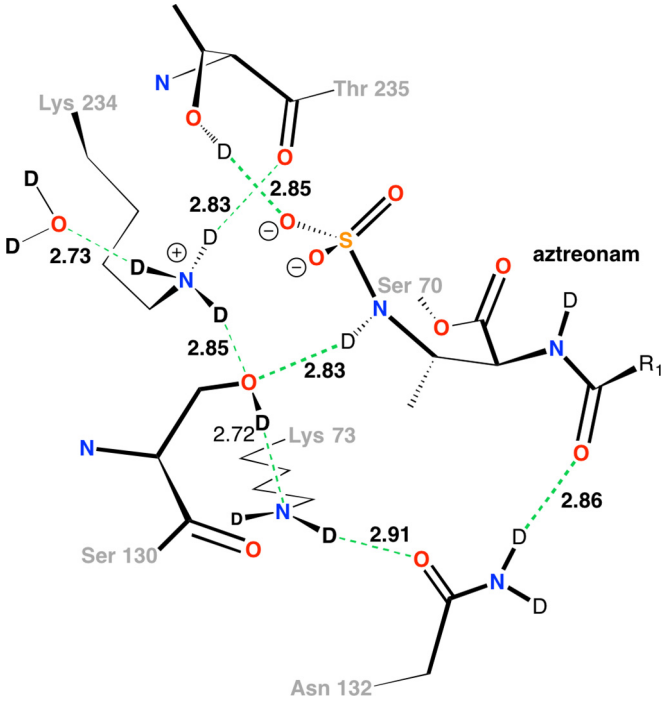

FIG 3 Hydrogen bonding network in the active site. All distances (between donor and acceptor heavy atoms [indicated in angstroms]) are from the 15 K acyl-enzyme intermediate X-ray structure.

Å) (Fig. 2C). The omit electron density for D_γ of Ser 130 indicates that it is orientated toward N_ζ of Lys 73 (Fig. 2D), with which it forms a hydrogen bond (2.72 Å). The inferred details of these interactions within the active site are shown in Fig. 3. Several other interactions between the monobactam and the protein are also present. The main chain carbonyl of Ser 237 hydrogen bonds to an amide group of the monobactam (2.77 Å), while one of the dual conformations of the side chain of Ser 237 interacts with a carboxylate group on the monobactam (2.70 Å). The carbonyl group of the monobactam also forms interactions with the amino groups of Asn 104 (3.00 Å) and Asn 132 (2.87 Å).

The 293 K neutron diffraction data are very similar to the 15 K X-ray structure data in that Lys 234 is present in the ND_3^+ form and the D_γ atom of Ser 130 is oriented toward Lys 73. However, in deuterium omit maps, the neutron structure clearly shows that Lys 73 is in the neutral ND_2 form (Fig. 4) and is hydrogen bonded to O_δ of Asn 132.

Several investigators have proposed roles for both Lys 73 and Ser 130 in the protonation of the β-lactam ring nitrogen (11, 14, 24–26). The closest proton source to the β-lactam nitrogen is the hydroxyl group of Ser 130, but until now it has not been clear whether Lys 234 or Lys 73 acts as the proton source to complete the acylation step in the catalytic mechanism. The observed protonation states of Lys 234 ($-ND_3^+$) and Lys 73 ($-ND_2$) from our neutron and X-ray structures indicate that Lys 73 is the proton source, as previously suggested (11, 14, 27). In the Glu 166 Ala mutant, the Lys 73 side chain most likely acts as a general base in the acylation reaction, having extracted a proton from Ser 70. A second proton transfer pathway would initiate the transfer of two protons. The first proton would be transferred from N_ζ of Lys 73 to O_γ of Ser 130, and the second proton would be transferred from O_γ of Ser 130 to the β-lactam nitrogen, thereby leaving Lys 73 in the $-ND_2$ neutral form observed in our X-ray and neutron structures. The ability of Glu 166 Ala mutants to form acyl-enzyme intermediates indicates that Lys 73 is able to act as a general base in the acylation part of the reaction, as supported by enzyme kinetics measurements (15, 28). However, the large drop in the acylation rate of the Glu 166 Ala mutant clearly shows that Glu 166 takes part in the acylation step in which it has also been proposed to act as the general base (12, 13, 29).

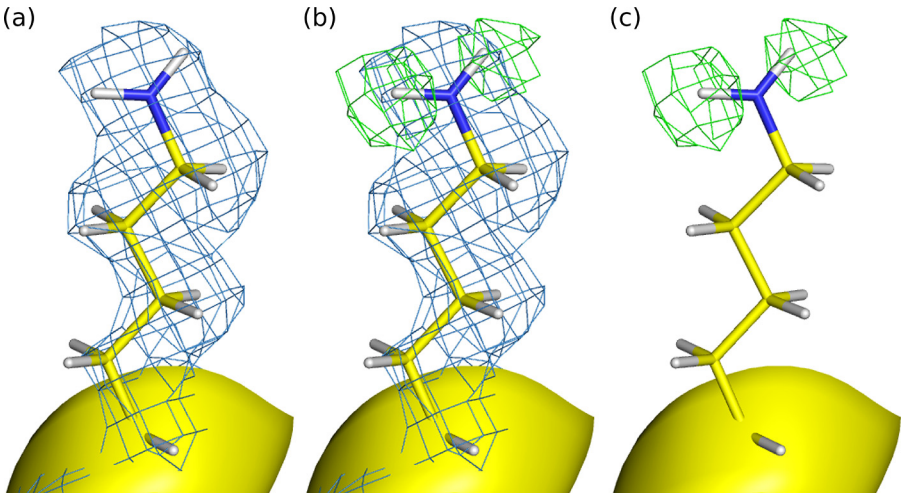

FIG 4 The neutron data uniquely reveal that Lys 73 is in the neutral ND_2 protonation state. (a) The $2F_o$-F_c 293 K nuclear density map (blue mesh) is contoured at 1.5 σ. (b) The $2F_o$-F_c 293 K nuclear density map (blue mesh) is contoured at 1.5 σ, and the deuterium omit difference density map (green mesh) is contoured at 1.5 σ for the left deuterium atom and +1.2 σ for the right deuterium atom. (c) The deuterium omit difference density map (green mesh) is contoured as described for panel b.

On the basis of quantum mechanical/molecular mechanical (QM/MM) calculations, the Glu 166 Ala mutation was proposed to lower the pK_a of Lys 73, enabling it to act as a general base during the acylation step (14, 17). Our structures show direct (and indirect) evidence that the mutation of Glu 166 to Ala alters the pK_a of Lys 73, possibly reverting the enzyme to a penicillin-binding protein capable of binding β-lactams but incapable of releasing them. The presence of an acylated aztreonam within the active site is also likely to affect the pK_a values of the catalytic residues.

Previous studies by Gibson et al. (19) have shown that the Lys 73 Arg mutant shows a 100-fold lower rate for the acylation reaction and that a dual Lys 73 Arg/Glu 166 Asp mutant shows a 10,000-fold lower rate. Thus, the dual presence and interaction of both Glu 166 and Lys 73 are vital in the acylation mechanism of the class A β-lactamase enzymes for which both amino acids are required for catalytic competency.

Conclusions. Using both X-ray and neutron crystallography, we have located the positions of most of the hydrogen (deuterium) atoms within the active site of Toho-1 β-lactamase in its acyl-enzyme intermediate state in complex with aztreonam. These structures suggest that Lys 73 can act as a general base in the acylation step of the β-lactam hydrolysis reaction, as has been previously proposed (11, 14, 17, 30). The experimentally observed deuterium positions seen in our neutron and X-ray structures are a match to those put forward by Mobashery and coworkers from their studies on TEM-1 β-lactamase in which they used different techniques (QM/MM and nuclear magnetic resonance [NMR]) with a different substrate and yet determined the same protonation states (14, 17). This indicates that these results, which have been verified by four different techniques, are broadly applicable to class A β-lactamase catalysis.

MATERIALS AND METHODS

Perdeuteration is the complete replacement of hydrogen with deuterium, which dramatically increases the signal-to-noise ratio of neutron diffraction data while also enabling the experimental location of all the atoms in the protein (21, 22, 31). Using perdeuterated protein crystals, neutron diffraction data on the Glu 166 Ala/Arg 274 Asn/Arg 276 Asn Toho-1 β-lactamase aztreonam acyl-enzyme intermediate were collected on the macromolecular neutron diffractometer (MaNDi) beamline at the Spallation Neutron Source (32, 33). A perdeuterated protein crystal roughly 0.9 mm^3 in volume was placed for 2 to 3 h in a reservoir D_2O solution containing 2.7 M ammonium sulfate, 0.1 M sodium citrate (pH 6.1), and 5.0 mM aztreonam. The crystal was then sealed in a quartz capillary for neutron data collection on MaNDi using neutrons with wavelengths between 2 to 4 Å to collect a series of time of flight wavelength-resolved Laue diffraction images. A total of 10 wavelength-resolved Laue diffraction images were collected with a 6-h exposure time per image. Between images, the sample was rotated by 10 degrees on the ϕ axis. In addition to neutron diffraction data, we also collected a 15 K X-ray diffraction data set

on a smaller perdeuterated protein crystal to beyond atomic resolution (1.10 Å) on the SBC-CAT sector 19 beamline at the Advanced Photon Source (APS). High-resolution monochromatic (0.67-Å) X-ray diffraction data were collected on the acyl-enzyme complex using a Cryo Industries of America Cryocool helium cryostream at 15 K. The 15 K X-ray data were processed using the XDS (34) package, whereas the neutron data were processed using the Mantid package (35) and the Lauenorm program from the Lauegen package (36). Lauenorm was then used for wavelength normalization of the Laue data and scaling between Laue diffraction images. The PHENIX suite (37) was used to refine the 293 K neutron and 15 K X-ray data to convergence separately. Further refinement was done on the neutron data using Shelx (38), and all model building was done using the Coot (39) molecular graphics program. The data reduction and refinement statistics for the two structures are given in File S1 of the supplemental material.

Accession number(s). Experimental data and coordinates were deposited with PDB identifiers 5G18 and 5KSC.

SUPPLEMENTAL MATERIAL

Supplemental material for this article may be found at https://doi.org/10.1128/AAC.01636-16.

TEXT S1, PDF file, 0.2 MB.

ACKNOWLEDGMENTS

This research was sponsored by the Laboratory Directed Research and Development Program at Oak Ridge National Laboratory (ORNL), which is managed by UT-Battelle, LLC, for the U.S. Department of Energy (DOE). Research at ORNL's Spallation Neutron Source was sponsored by the Scientific User Facilities Division, Office of Basic Energy Sciences, U.S. Department of Energy. The Office of Biological and Environmental Research supported research at Oak Ridge National Laboratory's Center for Structural Molecular Biology (CSMB), using facilities supported by the Scientific User Facilities Division, Office of Basic Energy Sciences, U.S. Department of Energy. Results shown in this report are derived from work performed at Argonne National Laboratory (ANL), Structural Biology Center at the Advanced Photon Source. ANL is operated by UChicago Argonne, LLC, for the U.S. Department of Energy, Office of Biological and Environmental Research, under contract DE-AC02-06CH11357.

REFERENCES

1. Drawz SM, Bonomo RA. 2010. Three decades of beta-lactamase inhibitors. Clin Microbiol Rev 23:160–201. https://doi.org/10.1128/CMR.00037-09.
2. Fisher JF, Meroueh SO, Mobashery S. 2005. Bacterial resistance to β-lactam antibiotics: compelling opportunism, compelling opportunity. Chem Rev 105:395–424. https://doi.org/10.1021/cr030102i.
3. Bonnet R. 2004. Growing group of extended-spectrum beta-lactamases: the CTX-M enzymes. Antimicrob Agents Chemother 48:1–14. https://doi.org/10.1128/AAC.48.1.1-14.2004.
4. Ambler RP, Coulson AF, Frère JM, Ghuysen JM, Joris B, Forsman M, Levesque RC, Tiraby G, Waley SG. 1991. A standard numbering scheme for the class A beta-lactamases. Biochem J 276:269–270. https://doi.org/10.1042/bj2760269.
5. Matagne A, Lamotte-Brasseur J, Frère JM. 1998. Catalytic properties of class A beta-lactamases: efficiency and diversity. Biochem J 330:581–598. https://doi.org/10.1042/bj3300581.
6. Knox JR. 1995. Extended-spectrum and inhibitor-resistant TEM-type beta-lactamases: mutations, specificity, and three-dimensional structure. Antimicrob Agents Chemother 39:2593–2601. https://doi.org/10.1128/AAC.39.12.2593.
7. Ibuka A, Taguchi A, Ishiguro M, Fushinobu S, Ishii Y, Kamitori S, Okuyama K, Yamaguchi K, Konno M, Matsuzawa H. 1999. Crystal structure of the E166A mutant of extended-spectrum beta-lactamase Toho-1 at 1.8 A resolution. J Mol Biol 285:2079–2087. https://doi.org/10.1006/jmbi.1998.2432.
8. Ishii Y, Ohno A, Taguchi H, Imajo S, Ishiguro M, Matsuzawa H. 1995. Cloning and sequence of the gene encoding a cefotaxime-hydrolyzing class A beta-lactamase isolated from Escherichia coli. Antimicrob Agents Chemother 39:2269–2275. https://doi.org/10.1128/AAC.39.10.2269.
9. Nitanai Y, Shimamura T, Uchiyama T, Ishii Y, Takehira M, Yutani K, Matsuzawa H, Miyano M. 2010. The catalytic efficiency (kcat/Km) of the class A beta-lactamase Toho-1 correlates with the thermal stability of its catalytic intermediate analog. Biochim Biophys Acta 1804:684–691. https://doi.org/10.1016/j.bbapap.2009.10.023.
10. Herzberg O, Moult J. 1987. Bacterial resistance to beta-lactam antibiotics: crystal structure of beta-lactamase from Staphylococcus aureus PC1 at 2.5 A resolution. Science 236:694–701. https://doi.org/10.1126/science.3107125.
11. Strynadka NCJ, Adachi H, Jensen SE, Johns K, Sielecki A, Betzel C, Sutoh K, James MNG. 1992. Molecular structure of the acyl-enzyme intermediate in β-lactam hydrolysis at 1.7 Å resolution. Nature 359:700–705. https://doi.org/10.1038/359700a0.
12. Chen Y, Bonnet R, Shoichet BK. 2007. The acylation mechanism of CTX-M beta-lactamase at 0.88 a resolution. J Am Chem Soc 129:5378–5380. https://doi.org/10.1021/ja0712064.
13. Minasov G, Wang X, Shoichet BK. 2002. An ultrahigh resolution structure of TEM-1 beta-lactamase suggests a role for Glu166 as the general base in acylation. J Am Chem Soc 124:5333–5340. https://doi.org/10.1021/ja0259640.
14. Meroueh SO, Fisher JF, Schlegel HB, Mobashery S. 2005. Ab initio QM/MM study of class A beta-lactamase acylation: dual participation of Glu166 and Lys73 in a concerted base promotion of Ser70. J Am Chem Soc 127:15397–15407. https://doi.org/10.1021/ja051592u.
15. Guillaume G, Vanhove M, Lamotte-Brasseur J, Ledent P, Jamin M, Joris B, Frère J-M. 1997. Site-directed mutagenesis of glutamate 166 in two β-lactamases. Kinetic and molecular modeling studies. J Biol Chem 272:5438–5444. https://doi.org/10.1074/jbc.272.9.5438.
16. Imtiaz U, Billings E, Knox J, Manavathu E, Lerner S, Mobashery S. 1993. Inactivation of class-A beta-lactamases by clavulanic acid—the role of arginine-244 in a proposed nonconcerted sequence of events. J Am Chem Soc 115:4435–4442. https://doi.org/10.1021/ja00064a003.
17. Golemi-Kotra D, Meroueh SO, Kim C, Vakulenko SB, Bulychev A, Stem-

mler AJ, Stemmler TL, Mobashery S. 2004. The importance of a critical protonation state and the fate of the catalytic steps in class A beta-lactamases and penicillin-binding proteins. J Biol Chem 279: 34665–34673. https://doi.org/10.1074/jbc.M313143200.
18. Joris B, Ghuysen JM, Dive G, Renard A, Dideberg O, Charlier P, Frère JM, Kelly JA, Boyington JC, Moews PC. 1988. The active-site-serine penicillin-recognizing enzymes as members of the Streptomyces R61 DD-peptidase family. Biochem J 250:313–324. https://doi.org/10.1042/bj2500313.
19. Gibson RM, Christensen H, Waley SG. 1990. Site-directed mutagenesis of β-lactamase I. Single and double mutants of Glu-166 and Lys-73. Biochem J 272:613–619.
20. Shimamura T, Nitanai Y, Uchiyama T, Matsuzawa H. 2009. Improvement of crystal quality by surface mutations of beta-lactamase Toho-1. Acta Crystallogr Sect F Struct Biol Cryst Commun 65:379–382. https://doi.org/10.1107/S1744309109008240.
21. Tomanicek SJ, Blakeley MP, Cooper J, Chen Y, Afonine PV, Coates L. 2010. Neutron diffraction studies of a class A beta-lactamase Toho-1 E166A/R274N/R276N triple mutant. J Mol Biol 396:1070–1080. https://doi.org/10.1016/j.jmb.2009.12.036.
22. Tomanicek SJ, Wang KK, Weiss KL, Blakeley MP, Cooper J, Chen Y, Coates L. 2011. The active site protonation states of perdeuterated Toho-1 β-lactamase determined by neutron diffraction support a role for Glu166 as the general base in acylation. FEBS Lett 585:364–368. https://doi.org/10.1016/j.febslet.2010.12.017.
23. Quon BS, Goss CH, Ramsey BW. 2014. Inhaled antibiotics for lower airway infections. Ann Am Thorac Soc 11:425–434. https://doi.org/10.1513/AnnalsATS.201311-395FR.
24. Lamotte-Brasseur J, Dive G, Dideberg O, Charlier P, Frère JM, Ghuysen JM. 1991. Mechanism of acyl transfer by the class A serine beta-lactamase of Streptomyces albus G. Biochem J 279:213–221. https://doi.org/10.1042/bj2790213.
25. Atanasov BP, Mustafi D, Makinen MW. 2000. Protonation of the β-lactam nitrogen is the trigger event in the catalytic action of class A β-lactamases. Proc Natl Acad Sci U S A 97:3160–3165. https://doi.org/10.1073/pnas.97.7.3160.
26. Thomas VL, Golemi-Kotra D, Kim C, Vakulenko SB, Mobashery S, Shoichet BK. 2005. Structural consequences of the inhibitor-resistant Ser130Gly substitution in TEM beta-lactamase. Biochemistry 44:9330–9338. https://doi.org/10.1021/bi0502700.
27. Vandavasi VG, Weiss KL, Cooper JB, Erskine PT, Tomanicek SJ, Ostermann A, Schrader TE, Ginell SL, Coates L. 2016. Exploring the mechanism of β-lactam ring protonation in the class A β-lactamase acylation mechanism using neutron and X-ray crystallography. J Med Chem 59:474–479. https://doi.org/10.1021/acs.jmedchem.5b01215.
28. Knox JR, Moews PC, Escobar WA, Fink AL. 1993. A catalytically-impaired class A beta-lactamase: 2 A crystal structure and kinetics of the Bacillus licheniformis E166A mutant. Protein Eng 6:11–18. https://doi.org/10.1093/protein/6.1.11.
29. Escobar WA, Tan AK, Lewis ER, Fink AL. 1994. Site-directed mutagenesis of glutamate-166 in beta-lactamase leads to a branched path mechanism. Biochemistry 33:7619–7626. https://doi.org/10.1021/bi00190a015.
30. Maveyraud L, Pratt RF, Samama JP. 1998. Crystal structure of an acylation transition-state analog of the TEM-1 beta-lactamase. Mechanistic implications for class A beta-lactamases. Biochemistry 37:2622–2628.
31. Tomanicek SJ, Standaert RF, Weiss KL, Ostermann A, Schrader TE, Ng JD, Coates L. 2013. Neutron and X-ray crystal structures of a perdeuterated enzyme inhibitor complex reveal the catalytic proton network of the Toho-1 beta-lactamase for the acylation reaction. J Biol Chem 288: 4715–4722. https://doi.org/10.1074/jbc.M112.436238.
32. Coates L, Cuneo MJ, Frost MJ, He J, Weiss KL, Tomanicek SJ, McFeeters H, Vandavasi VG, Langan P, Iverson EB. 2015. The macromolecular neutron diffractometer MaNDi at the Spallation Neutron Source. J Appl Crystallogr 48:1302–1306. https://doi.org/10.1107/S1600576715011243.
33. Coates L, Stoica AD, Hoffmann C, Richards J, Cooper R. 2010. The macromolecular neutron diffractometer (MaNDi) at the Spallation Neutron Source, Oak Ridge: enhanced optics design, high-resolution neutron detectors and simulated diffraction. J Appl Crystallogr 43:570–577. https://doi.org/10.1107/S0021889810008587.
34. Kabsch W. 2010. *XDS*. Acta Crystallogr D Biol Crystallogr 66:125–132. https://doi.org/10.1107/S0907444909047337.
35. Arnold O, Bilheux JC, Borreguero JM, Buts A, Campbell SI, Chapon L, Doucet M, Draper N, Ferraz Leal R, Gigg MA, Lynch VE, Markvardsen A, Mikkelson DJ, Mikkelson RL, Miller R, Palmen K, Parker P, Passos G, Perring TG, Peterson PF, Ren S, Reuter MA, Savici AT, Taylor JW, Taylor RJ, Tolchenov R, Zhou W, Zikovsky J. 2014. Mantid—data analysis and visualization package for neutron scattering and SR experiments. Nucl Instrum Methods Phys Res A 764:156–166. https://doi.org/10.1016/j.nima.2014.07.029.
36. Campbell JW, Hao Q, Harding MM, Nguti ND, Wilkinson C. 1998. LAUEGEN version 6.0 and INTLDM. J Appl Crystallogr 31:496–502. https://doi.org/10.1107/S0021889897016683.
37. Adams PD, Afonine PV, Bunkóczi G, Chen VB, Davis IW, Echols N, Headd JJ, Hung L-W, Kapral GJ, Grosse-Kunstleve RW, McCoy AJ, Moriarty NW, Oeffner R, Read RJ, Richardson DC, Richardson JS, Terwilliger TC, Zwart PH. 2010. PHENIX: a comprehensive Python-based system for macromolecular structure solution. Acta Crystallogr D Biol Crystallogr 66:213–221. https://doi.org/10.1107/S0907444909052925.
38. Gruene T, Hahn HW, Luebben AV, Meilleur F, Sheldrick GM. 2014. Refinement of macromolecular structures against neutron data with SHELXL2013. J Appl Crystallogr 47:462–466. https://doi.org/10.1107/S1600576713027659.
39. Emsley P, Lohkamp B, Scott WG, Cowtan K. 2010. Features and development of Coot. Acta Crystallogr D Biol Crystallogr 66:486–501. https://doi.org/10.1107/S0907444910007493.